

# QCRS: Improve Randomized Smoothing using Quasi-Concave Optimization

Bo-Han Kung and Shang-Tse Chen

Department of Computer Science and Information Engineering, National Taiwan University

{d10922019, stchen}@csie.ntu.edu.tw

## Abstract

Randomized smoothing is currently the state-of-the-art method that provides certified robustness for deep neural networks. However, it often cannot achieve an adequate certified region on real-world datasets. One way to obtain a larger certified region is to use an input-specific algorithm instead of using a fixed Gaussian filter for all data points. Several methods based on this idea have been proposed, but they either suffer from high computational costs or gain marginal improvement in certified radius. In this work, we show that by exploiting the quasiconvex problem structure, we can find the optimal certified radii for most data points with slight computational overhead. This observation leads to an efficient and effective input-specific randomized smoothing algorithm. We conduct extensive experiments and empirical analysis on Cifar10 and ImageNet. The results show that the proposed method significantly enhances the certified radii with low computational overhead.

## 1 Introduction

Although deep learning has achieved tremendous success in various fields [Wang *et al.*, 2022; Zhai *et al.*, 2022], it is known to be vulnerable to adversarial attacks [Szegedy *et al.*, 2013]. This kind of attack crafts an imperceptible perturbation on images [Goodfellow *et al.*, 2014] or voices [Carlini and Wagner, 2018] to make the AI system predict incorrectly. Many adversarial defense methods have been proposed to defend against adversarial attacks. Adversarial defenses can be categorized into empirical defenses and theoretical defenses. Common empirical defenses include adversarial training [Madry *et al.*, 2017; Shafahi *et al.*, 2019; Wong *et al.*, 2020] and preprocessing-based methods [Samangouei *et al.*, 2018; Das *et al.*, 2018]. Though effective, empirical defenses cannot guarantee robustness.

Different from empirical defenses, theoretical defenses (certified defense), such as mixed-integer programming [Tjeng *et al.*, 2018], interval bound propagation [Ehlers, 2017; Gowal *et al.*, 2018], and randomized smoothing [Cohen *et al.*, 2019; Lecuyer *et al.*, 2019; Yang *et al.*, 2020],

can provide provable defense that theoretically and quantitatively guarantee robustness. The guarantee ensures that there are no adversarial examples within a specific ball with a radius  $r$ . Among these methods, only randomized smoothing (RS) can scale to state-of-the-art deep neural networks and real-world datasets. Randomized smoothing first builds a smoothed classifier for a given data point via a Gaussian filter and Monte Carlo sampling, and then it estimates a confidence lower bound for the highest-probability class. Next, it determines a certified region for the class and promise that there is no adversarial example within this region.

Although randomized smoothing is effective, it suffers from two main disadvantages. First, randomized smoothing applies the same constant-variance Gaussian filter to every data point when constructing a smoothed classifier. This makes the certified region dramatically underestimated. Second, randomized smoothing adopts a confidence lower bound (Clopper-Pearson lower bound) to estimate the highest-probability class, which also limits the certified region. As a result, when evaluating radius-accuracy curve, a truncation fall often occurs (see the gray curve in the upper right of Fig. 1). This is called truncation effect or waterfall effect [Súkeník *et al.*, 2021], which shows the conservation aspect in randomized smoothing. Other issues such as fairness [Mohapatra *et al.*, 2021], dimension [Kumar *et al.*, 2020b], and time-efficiency [Chen *et al.*, 2022] also limit the application of randomized smoothing.

To alleviate truncation effect and improve the certified radii, a more precise workflow is necessary. Prior work [Chen *et al.*, 2021; Alfarra *et al.*, 2022] proposed input-specific methods that can assign different Gaussian filters to different data points. Those methods attempt to optimize the radius by finding the optimal variance  $\sigma^2$  of the Gaussian filter. In this work, we first delve into randomized smoothing and discover a useful property called quasiconcavity for the sigma-radius curve. Next, based on quasiconcavity, we develop a novel algorithm called **Quasiconvexity-based Randomized Smoothing (QCRS)** that optimizes certified radii with respect to sigma. The overview of QCRS is illustrated in Fig. 1. QCRS significantly improves the certified region with little computational overhead compared to existing methods [Chen *et al.*, 2021; Alfarra *et al.*, 2022]. The proposed QCRS enjoys the advantages of both performance and time-efficiency. The main technical contributions are summarized as follows:

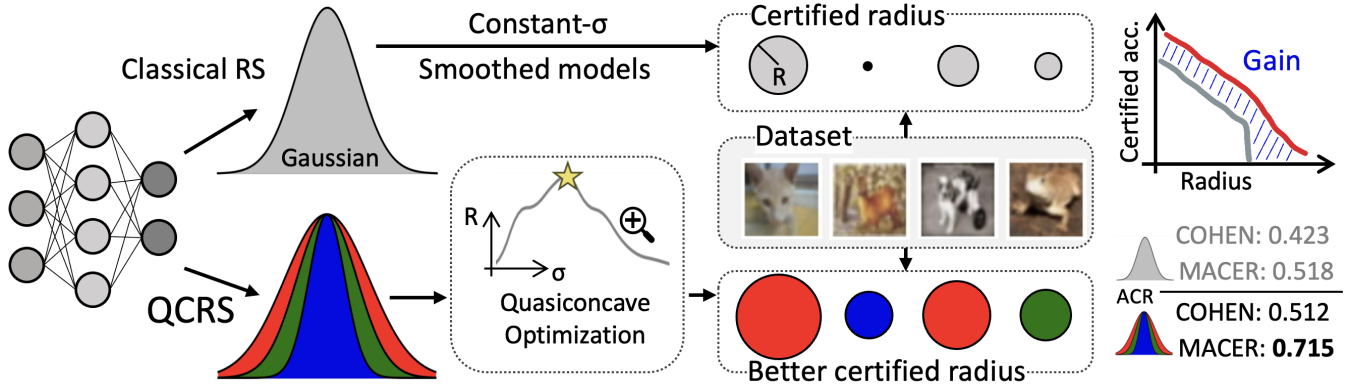


Figure 1: Overview of the proposed QCRS algorithm. QCRS finds the better sigma value for each smoothed classifier using quasiconcave optimization. Thus, it provides better certified regions than the classical randomized smoothing. In this paper, we discuss quasiconcavity on the certified radius w.r.t.  $\sigma$ , i.e.,  $R(\sigma)$ .

- We discover and prove that the sigma-radius curves are quasiconcave for most data points. In addition, we also show that the necessary condition for quasiconcavity is more general and easier to satisfy than the conditions proposed by prior work. In our experiments, approximately 99% of the data points satisfy our proposed quasiconcavity condition.
- Based on the observed quasiconcavity property, we propose a novel and efficient input-specific algorithm QCRS to improve the traditional randomized smoothing. QCRS enhances the certified radii and alleviates the truncation effect.
- Through extensive experiments, we demonstrate the effectiveness of our proposed QCRS method on the CIFAR-10 and ImageNet datasets. Furthermore, by combining QCRS with a training-based method, we achieve state-of-the-art certified radii.

## 2 Related Work

Randomized smoothing utilizes a spatial low-pass Gaussian filter to construct a smoothed model [Cohen *et al.*, 2019]. Based on the Neyman-Pearson lemma, this smoothed model can provide a provable radius  $r$  to guarantee robustness for large-scale datasets. To improve randomized smoothing, some works [Yang *et al.*, 2020; Zhang *et al.*, 2020; Levine and Feizi, 2021] proposed general methods using different smoothing distribution for different  $\ell_p$  balls, while others tried to provide a better and tighter certification [Kumar *et al.*, 2020a; Levine *et al.*, 2020].

**Improving RS during training phase.** To further enlarge the radius  $r$ , some works used training-based method [Salman *et al.*, 2019; Zhai *et al.*, 2019; Jeong *et al.*, 2021; Anderson and Sojoudi, 2022]. These models were specifically designed for randomized smoothing. For example, MACER [Zhai *et al.*, 2019] made the computation of certified radius differentiable and add it to the standard cross-entropy loss. Thus, the average certified radius of MACER outperforms the Gaussian-augmentation model that was used by the

original randomized smoothing [Cohen *et al.*, 2019].

**Improving RS during inference phase.** Different from training-based method, some works utilized different smoothing methods to enhance the certified region. Chen *et al.*, [2021] proposed a multiple-start search algorithm to find the best parameter for building smoothed classifiers. Alfarrar *et al.*, [2022] adopted a memory-based approach to optimize the Gaussian filter of each input data. Chen *et al.*, [2022] proposed an input-specific sampling acceleration method to control the sampling number and provides fast and effective certification. Li *et al.*, [2022] proposed double sampling randomized smoothing that utilizes additional smoothing information for tighter certification. These inference-time methods are the most relevant to our work. See Section 4.1 for more detailed description on these methods.

## 3 Preliminaries

Let  $x \in \mathbb{R}^d$  be a data point, where  $d$  is the input dimension.  $\mathcal{C} = \{1, 2, \dots, c\}$  is the set of classes.  $F : \mathbb{R}^d \rightarrow \mathbb{R}^c$  is a general predictor such as neural networks. We define the base classifier as

$$f(x) = e_\xi; \quad \xi = \arg \max_j F_j(x), \quad (1)$$

where  $e_j$  denotes a one-hot vector where the  $j^{\text{th}}$  component is 1 and all the other components are 0. The smoothed classifier [Cohen *et al.*, 2019]  $g : \mathbb{R}^d \rightarrow \mathcal{C}$  is defined as

$$g(x) = \arg \max_{c \in \mathcal{C}} Pr[f(x + \epsilon) = e_c], \quad \epsilon \sim \mathcal{N}(0, \sigma^2 I), \quad (2)$$

where  $\mathcal{N}$  is Gaussian distribution and  $\epsilon$  is a noise vector sampled from  $\mathcal{N}$ .

Cohen *et al.*, (COHEN) proposed a provable method to calculate the certifiable robust region as follows:

$$R = \frac{\sigma}{2} \cdot [\Phi^{-1}(p_A) - \Phi^{-1}(\overline{p_B})], \quad p_A = Pr[f(x + \epsilon) = e_A] \\ \text{and } p_B = Pr[f(x + \epsilon) = e_B], \quad (3)$$

where  $A$  is the highest-probability class of the smoothed classifier, and  $B$  is the runner-up class.  $\underline{p}_A$  and  $\overline{p}_B$  are the Clopper-Pearson lower/upper bound of  $p_A$  and  $p_B$ , which can be estimated by Monte Carlo (MC) sampling with a confidence level  $1 - \alpha$ .  $R$  indicates the certified radius. That is, any data point inside this region would be predicted as class  $A$  by the smoothed classifier. In practice, COHEN replaces  $\overline{p}_B$  with  $1 - \underline{p}_A$ , so equation 3 usually is reformulated as  $R = \sigma \cdot \Phi^{-1}(\underline{p}_A)$ . If  $\underline{p}_A < 0.5$ , it indicates that there is no certified region in this data point according to COHEN.

Randomized smoothing returns the highest-probability class predicted by the base classifier when perturbations  $\epsilon$  are added to  $x$ . Therefore, smoothed classifier  $g$  can be regarded as a spatial smoothing measure of the original base classifier using a Gaussian kernel  $\mathcal{G}$ , i.e.,  $f = g \star \mathcal{G}$ . Randomized smoothing constructs smoothed classifier to provide certifiable robustness guarantee.

## 4 QCRS Methodology

### 4.1 Observation and Motivation

Traditional randomized smoothing suffers from limited certified region and truncation effect, which degrade the certification performance. Several existing methods try to address these issues. Some focus on training the base model to enlarge certified radii, while others use a different Gaussian kernel  $\mathcal{G}$  for each image to construct  $g$ . We follow the later approach and propose an input-specific algorithm that finds the optimal  $\mathcal{G}$  for most data points. Intuitively, for a data point  $x$  of class  $y$ , if most neighboring points belong to the same class  $y$ , we can use  $\mathcal{G}$  with a larger variance to convolute  $x$ . In contrast, if the neighborhood is full of different class samples,  $\mathcal{G}$  needs a small variance to prevent misclassification. Below, we first describe some input-specific search algorithms used in prior work [Alfarra *et al.*, 2022; Chen *et al.*, 2021].

DDRS [Alfarra *et al.*, 2022] assumes that sigma-radius curves are concave and use gradient-based convex optimization along with some relaxation and approximation to find the  $\sigma$  value that provides maximum certified radii. However, in our observation, almost all sigma-radius curves are not concave. We randomly select 200 images from CIFAR-10 dataset and compute the certified radius with respect to  $\sigma$  for each image (Fig. 2). Among these 200 images, 164 of them can provide valid certified radii, and the other 36 images do not have certified regions. We check the concavity numerically for these 164 curves, i.e., check if  $\text{Hess}_\sigma(R) \leq 0$ ; unfortunately, only 11 images satisfy concavity. That is, 93.29% images are not concave. Thus, the gradient-based convex optimization method may not work well in this task.

Instead of depending on the assumption of concavity, InstaRS [Chen *et al.*, 2021] uses a multi-start searching algorithm to optimize  $\sigma$ . However, the multi-start procedure incurs high computational overhead. In our work, we observe an intriguing quasiconcave property on the sigma-radius curves, which helps us develop an effective and efficient algorithm to optimize sigma. As shown in Fig. 2, we plot the certified radii using standard RS (COHEN) under different values of  $\sigma$ . Due to expensive computation, we sample 20 values of  $\sigma$  at 0.15,

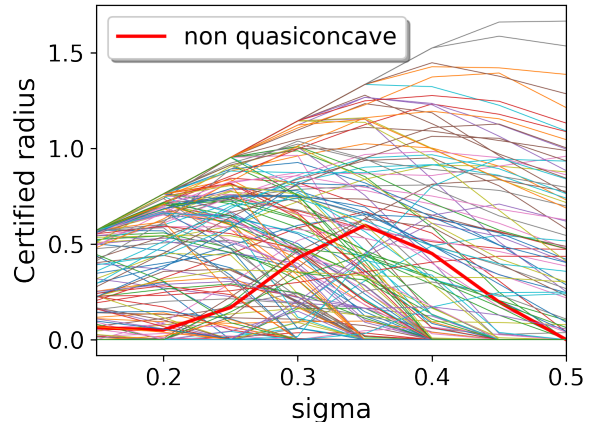


Figure 2: We evaluate the sigma-radius curves of 164 images from CIFAR-10 that can be certified by COHEN and check their concavity and quasiconcavity numerically. 6.7% and 99.4% of data points are concave and quasiconcave, respectively. The bold red curve is non-quasiconcave, and the others are all quasiconcave.

0.18, 0.2, 0.21, 0.22, 0.23, 0.24, 0.25, 0.26, 0.27, 0.28, 0.29, 0.3, 0.31, 0.32, 0.33, 0.35, 0.4, 0.45, and 0.5. Note that we increase the sampling density around  $\sigma = 0.25$  because this is the  $\sigma$  with which the model is trained. Next, we empirically verify the quasiconcavity of those curves. Since quasiconcavity is a much more general property than those used in prior work, we observe that only 1 out of the 164 curves we plot in Fig. 2 is non-quasiconcave. By utilizing the quasiconcave property, we design a more effective and efficient optimization algorithm than existing methods, which we describe in Subsection 4.3.

### 4.2 Quasiconvexity

This section lists the definition and two fundamental lemmas about quasiconcavity that will be used in designing our QCRS method. Quasiconvexity is a generalization of convexity, defined as follows:

**Definition 1.** (*quasiconvexity and quasiconcavity* [Boyd *et al.*, 2004]). *A function  $h$  is quasiconvex if  $\text{dom } h$  is convex and for any  $\theta \in [0, 1]$  and  $x, y \in \text{dom } h$ ,*

$$h(\theta x + (1 - \theta)y) \leq \max\{h(x), h(y)\}.$$

*Similarly, a function  $h$  is quasiconcave if*

$$h(\theta x + (1 - \theta)y) \geq \min\{h(x), h(y)\}.$$

*Furthermore, a function  $h$  is strictly quasiconvex if  $\text{dom } h$  is convex and for any  $x \neq y$ ,  $x, y \in \text{dom } h$ , and  $\theta \in (0, 1)$ :*

$$h(\theta x + (1 - \theta)y) < \max\{h(x), h(y)\}.$$

*Similarly, a function  $h$  is strictly quasiconcave if*

$$h(\theta x + (1 - \theta)y) > \min\{h(x), h(y)\}.$$

In this paper, we mainly use strict quasiconcavity. Below, we list lemmas on strict quasiconcavity that we will use later.

**Lemma 1.** *If a function  $h$  is strictly quasiconcave, then any local optimal solution of  $h$  must also be globally optimal.*

**Lemma 2.** *If  $h$  is strictly quasiconcave, and let  $x^*$  be the optimal solution. Then, the following two statements hold:*

$$\begin{aligned} \nabla h(x) &> 0, \text{ for } x \in (-\infty, x^*) \\ \nabla h(x) &< 0, \text{ for } x \in (x^*, \infty) \end{aligned}$$

### 4.3 Design

In this section, we show quasiconcavity related to sigma-radius curves. Consider  $R(\sigma) = \sigma \cdot \Phi^{-1}(\underline{p}_A(\sigma))$ . We want to get  $\sigma^* = \arg \max_{\sigma} R(\sigma)$ . This  $\sigma^*$  is the optimal solution to maximize  $R(\sigma)$ . First, we differentiate the objective  $R(\sigma)$ :

$$\begin{aligned} \nabla_{\sigma} R(\sigma) &= \frac{\partial R(\sigma)}{\partial \sigma} \\ &= \Phi^{-1}(\underline{p}_A(\sigma)) + \sigma \cdot \frac{\partial \Phi^{-1}(\underline{p}_A(\sigma))}{\partial \underline{p}_A(\sigma)} \cdot \frac{\partial \underline{p}_A(\sigma)}{\partial \sigma} \end{aligned} \quad (4)$$

According to Lemma 2, if equation 4 is positive for  $\sigma < \sigma^*$  and negative for  $\sigma > \sigma^*$ , the sigma-radius curve is strictly quasiconcave. However, there are some sigma values that can not be certified by randomized smoothing, i.e.,  $\{\sigma | \underline{p}_A(\sigma) < 0.5\}$ . We need to exclude these  $\sigma$  because the corresponding smoothed classifiers cannot provide certification. Therefore, we define a new condition based on Lemma 2 as follows:

**Definition 2.** ( $\sigma$ -SQC condition) *Given a  $\sigma^*$  that satisfies  $\nabla R(\sigma^*) = 0$  and  $R(\sigma^*) > 0$ , we call the sigma-radius curve satisfies  $\sigma$ -strict quasiconcave condition ( $\sigma$ -SQC condition), if for any  $\{\sigma | R(\sigma) > 0\}$ ,  $\nabla R(\sigma)$  satisfy the following:*

$$Pr_{\sigma < \sigma^*}[\nabla R(\sigma) > 0] + Pr_{\sigma > \sigma^*}[\nabla R(\sigma) < 0] = 2.$$

Intuitively,  $\sigma$ -SQC condition states that the slope of the sigma-radius curve is positive on the left side of the optimal solution and negative on the right side. Note that this condition is weaker and more general than the concentration assumption used in [Li *et al.*, 2022], which requires additional assumptions on the distribution of data points. It is also weaker than the concavity assumption used in DDRS [Alfarra *et al.*, 2022]. Since the  $\sigma$ -SQC condition is weaker, we expect that more data points would satisfy this assumption. In our experiment, roughly 99% of data points satisfy the  $\sigma$ -SQC condition, while only 6.7% of data points satisfy the concavity assumption [Alfarra *et al.*, 2022].

We assume that a data point satisfies  $\sigma$ -SQC condition. According to Lemma 2, if we detect that the gradient of a point is positive, we can assert that the optimal sigma is on its right hand side. Based on these rules, we design a time-efficient algorithm that can achieve optimal  $\sigma$ , shown in Algorithm 1. If the sigma-radius curve satisfies  $\sigma$ -SQC condition, Algorithm 1 finds the optimal sigma efficiently, which is the global optimal solution according to Lemma 1. On the other hand, the sigma values within the non-certified interval  $\{\sigma | R(\sigma) = 0\}$  must not be the solution. The gradients  $\nabla R(\sigma)$  are likely to be zero in the interval because the curve is a horizontal line with  $R(\sigma) = 0$  there. This leads to a gradient vanishing issue in Algorithm 1. To circumvent this issue, we utilize momentum  $M$  to guide the optimization direction. Algorithm 1 guarantees to find the same optimal solution as grid search if the curve satisfies  $\sigma$ -SQC condition. The time

---

### Algorithm 1 Bisection Randomized Smoothing

---

**Input:** Searching region  $\sigma_{max}$  and  $\sigma_{min}$ ; suboptimal interval  $\varepsilon$ ; original sigma  $\sigma_0$ ; gradient step  $\tau$

**Parameter:** momentum  $M \leftarrow 0$

**Output:** The optimal  $\sigma$

```

1: while  $\sigma_{max} - \sigma_{min} > \varepsilon$  do
2:    $\sigma \leftarrow (\sigma_{min} + \sigma_{max})/2$ 
3:   Calculate the gradient  $\nabla_{\sigma} R(\sigma) \leftarrow R(\sigma+\tau) - R(\sigma-\tau)$ 
4:   if  $sign(\nabla_{\sigma} R(\sigma)) > 0$  then
5:      $\sigma_{min} \leftarrow \sigma$ ;  $M \leftarrow 1$ 
6:   else if  $sign(\nabla_{\sigma} R(\sigma)) < 0$  then
7:      $\sigma_{max} \leftarrow \sigma$ ;  $M \leftarrow -1$ 
8:   else
9:     if  $M \geq 0$  then
10:       $\sigma_{max} \leftarrow \sigma$ ;  $M \leftarrow -1$ 
11:    else
12:       $\sigma_{min} \leftarrow \sigma$ ;  $M \leftarrow 1$ 
13:    end if
14:   end if
15: end while
16:  $\hat{\sigma} \leftarrow (\sigma_{min} + \sigma_{max})/2$ 
17: return  $\sigma \leftarrow \arg \max_{\sigma \in \{\hat{\sigma}, \sigma_0\}} R(\sigma)$ 

```

---

complexity is  $N$  for grid search and  $\log N$  for Algorithm 1, where  $N$  is the number of points on the grid. Therefore, the proposed method is significantly faster than grid search, while both of them can achieve the same optimal  $\sigma$ .

Prior work utilizes backpropagation to compute gradients, which is time-consuming, and the computed gradient is unstable due to MC sampling. Therefore, we use forward passes to compute gradient, which takes the difference of two neighboring points. This is because we only care about the gradient sign rather than the exact value. On the last stage of Algorithm 1, we employ a rejection policy that compares the resulting  $\sigma$  to the original  $\sigma$  and returns the larger one.

Thus, the proposed method is time-efficient compared to Insta-RS [Chen *et al.*, 2021] and DDRS [Alfarra *et al.*, 2022]. DDRS uses a low MC sampling number (one or eight) due to expansive computation and may obtain unstable gradients. To verify this, we analyze the value of gradient under different MC sampling number, and the results are shown in Fig. 3 (d). The gradient values vary dramatically when using low MC sampling numbers. Thus, a low MC sampling number may not accurately estimate gradients, which would affect the gradient-based optimization. On the other hand, the proposed QCRS only utilizes the gradient sign, which is much more stable than the gradient value as Fig. 3 (d) shows. The sign hardly changes when the MC sampling number exceeds 500.

### 4.4 Convergence Analysis

The proposed QCRS enjoys a convergence guarantee with the convergence rate analyzed below.

**Theorem 1.** *Given hyper-parameters  $\sigma_{min}$  and  $\sigma_{max}$ , let  $\sigma_t$  be the  $\sigma$  value after  $t$  iterations in Algorithm 1. Algorithm 1*

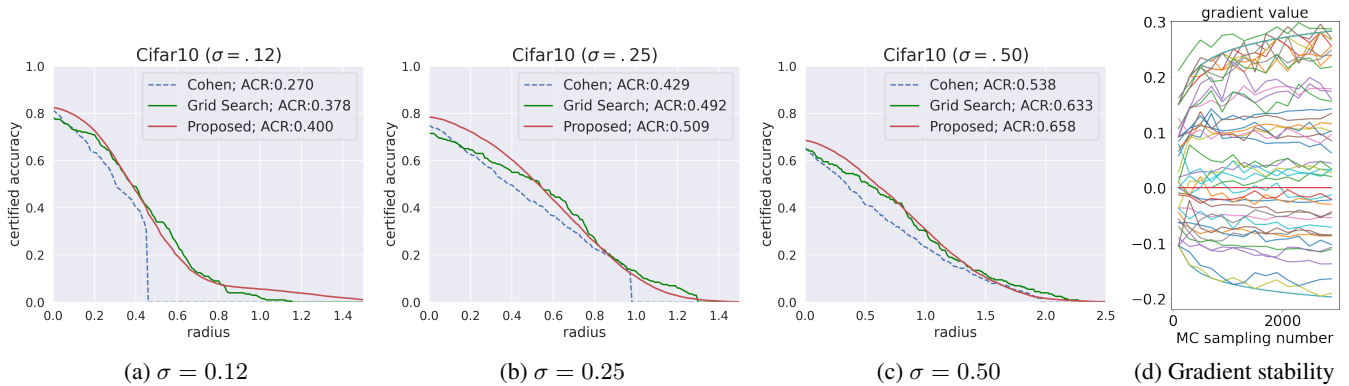


Figure 3: The comparison between COHEN, grid search, and the proposed QCRS on the CIFAR-10 dataset. The models are trained by Gaussian augmentation with sigma (a) 0.12, (b) 0.25, and (c) 0.50. The proposed QCRS outperforms the baseline method and is very close to grid search. In addition, we can observe the truncation effect on the curves of COHEN. (d) Gradient values with respect to different MC sampling numbers. The gradient values with regard to different MC sampling numbers are unstable, but their signs remain the same in almost all cases. The proposed QCRS is stable in the optimization as it only relies on the signs of gradient values.

converges to optimal  $\sigma^*$  as follows:

$$\frac{\sigma_{max} - \sigma_{min}}{2^t} \geq |\sigma_t - \sigma^*|,$$

which means the convergence rate of Algorithm 1 is  $\mathcal{O}((\frac{1}{2})^t)$ . We defer the proof to Appendix B.

On the other hand, gradient-descent-based method such as DDRS [Alfarra *et al.*, 2022] requires much stricter assumptions, such as L-smoothness and  $\mu$ -strongly concavity, to guarantee convergence. When these conditions are satisfied, the convergence rate is as below [Nesterov, 2018]:

$$|\sigma_t - \sigma^*|^2 \leq \left(\frac{L - \mu}{L + \mu}\right)^{(t-1)} |\sigma_1 - \sigma^*|^2.$$

The convergence rate is  $\mathcal{O}((\frac{L-\mu}{L+\mu})^t)$ , where  $L$  and  $\mu$  depend on the data points. Although these two convergence rates are incomparable, only 6.7% of data points satisfy the concavity assumption empirically, and even fewer data points satisfy L-smoothness and  $\mu$ -strongly concavity simultaneously. Thus, prior works [Chen *et al.*, 2021; Alfarra *et al.*, 2022] cannot converge to the optimal sigma values for most data points. In contrast, the proposed QCRS guarantees a fast  $\mathcal{O}((\frac{1}{2})^t)$  convergence rate if the  $\sigma$ -SQC condition holds. In our experiments, 99% of the data points satisfy the  $\sigma$ -SQC condition. Thus, the proposed QCRS compares favorably to prior work from the convergence perspective.

#### 4.5 Implementation Details

We use an NVIDIA GeForce® RTX 3090 GPU and an AMD Ryzen 5 5600X CPU with 32GB DRAM to run the experiments. Following prior work, we use ResNet10 for CIFAR-10 and ResNet50 for ImageNet. We use 500 as the MC sampling number to estimate gradients in Algorithm 1. The terminal condition of Algorithm 1 depends on  $\epsilon$ , which indicates an  $\epsilon$ -optimal solution, i.e.,  $|\sigma - \sigma^*| \leq \epsilon$ . The  $\epsilon$  we used in our experiments is 0.01, and  $\tau$  (the step to compute gradient) is  $\pm 0.05$ . Regarding grid search, we use 24 points for CIFAR-10 and 8 points for ImageNet. The searching region is 0.08

Table 1: ACR and Time Cost for CIFAR-10.

ACR	$\sigma = .12$	$\sigma = .25$	$\sigma = .50$	Time Cost (Sec.)
COHEN	0.270	0.429	0.538	6.50±0.021
Grid Search	0.378	0.492	0.633	155.80±0.50
<b>QCRS</b>	<b>0.400</b>	<b>0.509</b>	<b>0.658</b>	6.96±0.017

to 0.50 for  $\sigma = 0.12$ , 0.15 to 0.7 for  $\sigma = 0.25$ , and 0.25 to 1.0 for  $\sigma = 0.50$ .

## 5 Experimental Results

We evaluate the proposed QCRS and present the experimental results on CIFAR-10 [Krizhevsky *et al.*, 2009] and ImageNet [Russakovsky *et al.*, 2015]. We also verify that QCRS can be combined with training-based techniques like MACER [Zhai *et al.*, 2019] to produce state-of-the-art certification results. Following [Zhai *et al.*, 2019], we use the average certified radius (ACR) as the performance metric, defined as:  $ACR = \frac{1}{|\mathcal{D}_{test}|} \sum_{x \in \mathcal{D}_{test}} R(x, y; g)$ , where  $\mathcal{D}_{test}$  is the test dataset, and  $R(x, y; g)$  is the certified radius obtained by the smoothed classifier  $g$ .

### 5.1 CIFAR-10

Fig. 3 compares the radius-accuracy curves for different methods on the CIFAR-10 dataset. In the figure, we also show the corresponding ACR, which is the area under the radius-accuracy curve. Table 1 presents the ACR of different methods and their runtime cost. The proposed QCRS outperforms the original randomized smoothing method [Cohen *et al.*, 2019] by significant margins: 48%, 18%, and 22% for  $\sigma = \{0.12, 0.25, 0.50\}$ , respectively. The main performance gain comes from reducing the truncation effect (the waterfall effect) on the radius-accuracy curve. We also compare QCRS to grid search and show the results in Fig. 3. The number of searching points is 24 for each grid search. Since grid search is extremely computationally expensive, we only test the images with  $id = 0, 49, 99, \dots, 9999$  in CIFAR-10. Despite us-



Table 2: Certified accuracy under different radii  $r$  of DSRS, DDSRS, Grid Search, and the proposed QCRS. (“+%” indicates the relative improvement compared to COHEN.)

Certified radii $r$	Certified Accuracy								
	0.25	0.5	0.75	1.0	1.25	1.5	1.75	2.0	2.25
COHEN [Li <i>et al.</i> , 2022]	0.56	0.41	0.28	0.19	0.15	0.10	0.08	0.04	0.02
+DSRS [Li <i>et al.</i> , 2022] (+%)	0.57	0.43	0.31	0.21	0.16	0.13	0.08	0.06	0.04
	1.8%	4.9%	10.7%	10.5%	6.7%	30.0%	0.0%	50%	100%
COHEN [Alfarra <i>et al.</i> , 2022]	0.58	0.40	0.29	0.20	0.13	0.07	0.03	0.00	0.00
+DDRS [Alfarra <i>et al.</i> , 2022] (+%)	0.65	0.48	0.38	0.28	0.17	0.08	0.03	0.01	0.00
	12.1%	20.0%	31.0%	<b>40.0%</b>	30.8%	14.3%	0.0%	NA	0.0%
COHEN (Ours)	0.55	0.41	0.32	0.23	0.15	0.09	0.05	0.00	0.00
+Grid Search (24 points) (+%)	0.58	0.51	0.42	0.30	0.18	0.12	0.07	0.04	0.01
	5.5%	24.4%	31.2%	30.4%	20.0%	<b>33.3%</b>	<b>40%</b>	NA	NA
COHEN (Ours)	0.55	0.41	0.32	0.23	0.15	0.09	0.05	0.00	0.00
+QCRS (Proposed) (+%)	0.64	0.54	0.43	0.31	0.20	0.11	0.05	0.02	0.01
	<b>16.4%</b>	<b>31.7%</b>	<b>34.4%</b>	34.8%	<b>33.3%</b>	22.2%	0.0%	NA	NA

ing 24 points in the grid search, which costs approximately 24 times more in runtime than QCRS, QCRS still outperforms grid search. This is because QCRS is more efficient in terms of time, allowing for a larger searching region than in grid search. Furthermore, QCRS guarantees to achieve the same optimal as grid search if the  $\sigma$ -SQC condition holds. Regarding the computational cost, the proposed method only takes about 7% additional inference time compared to the original COHEN method, as shown in Table 1.

We also compare the proposed QCRS with two state-of-the-art randomized smoothing methods, DSRS [Li *et al.*, 2022] and DDSRS [Alfarra *et al.*, 2022]. We follow their setting to evaluate the proposed method for fair comparisons. However, randomized smoothing has random components such as MC sampling, and different works may have subtle parameter selection differences. Although these factors do not affect the results significantly, they still cause small variances in the certification results. Thus, we present the original COHEN baseline results reported in the two papers that we compare to and demonstrate their relative improvement for fair comparisons (Table 2). We can see that the original Cohen’s result from these works are different but close. We demonstrate the relative improvement on the certified accuracies under different radii of DSRS and DDSRS. As Table 2 shows, for the certified accuracy under radius at 0.5, DSRS and DDSRS improve COHEN by 4.9% and 20.0%, respectively. On the other hand, the proposed QCRS improves COHEN by 31.7%. Therefore, among the methods that boost certified radii, QCRS improves COHEN most effectively.

## 5.2 ImageNet

Fig. 4 shows the results on ImageNet.<sup>1</sup> Following [Cohen *et al.*, 2019], only 500 images with  $id = 0, 99, 199, \dots, 49999$  in the validation set were used. For the model with  $\sigma = .25$ , the proposed method improves ACR from 0.477 to 0.541, roughly 13.4%. Similarly, for the model with  $\sigma = .50$ , the proposed method improves ACR from 0.733 to 0.805,

<sup>1</sup>We did not use the model with  $\sigma = 1.0$ . This is because [Mohapatra *et al.*, 2021] has proven that a large  $\sigma$  causes serious fairness issues, and thus  $\sigma$  must be limited in randomized smoothing.

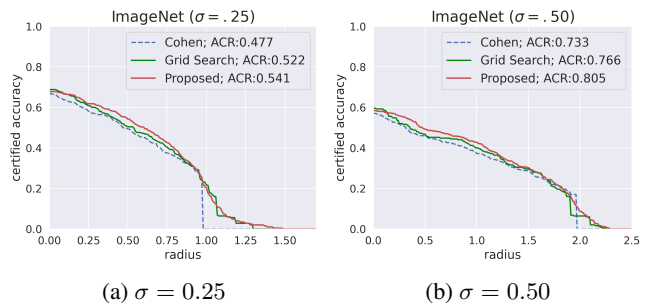


Figure 4: The comparison between COHEN, grid search, and the proposed QCRS on ImageNet. Following Cohen, we only use 500 images in the validation set. The models are trained by Gaussian augmentation with sigma (a) 0.25 and (b) 0.50.

roughly 9.8%. In addition, the proposed method overcomes the truncation effect, providing a larger certified radius compared to COHEN. As for the grid search, similar to CIFAR-10, it is computationally expensive, so we set the number of searching points to be 11 on ImageNet. As mentioned earlier, although the grid search can provide the optimal certified radius if the cost does not matter, its searching region and precision are limited in practical application. That is why the proposed method achieves a slightly superior ACR than the brute-force grid search method in Fig. 4, while the runtime is more than 8 times faster than the grid search.

## 5.3 MACER

The proposed method focuses on enhancing randomized smoothing while building the smoothed classifier. Thus, it is orthogonal to the approach that aims to boost certified radii during training stage. We evaluate QCRS on different training weight. QCRS can incorporate with training-based methods. The most representative training-based method to enhance certified radius is MACER. We apply the proposed method to models trained by MACER and observe significant improvement in terms of the certified radius. Fig. 5 illustrates the results, and Table 3 shows the detailed cross

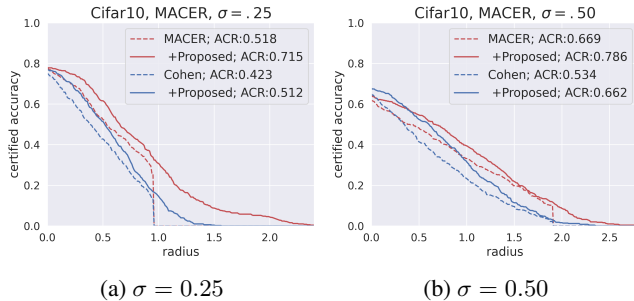


Figure 5: The performance of QCRS incorporating training-based methods. We use MACER model with (a)  $\sigma = 0.25$  and (b)  $\sigma = 0.50$ . Both QCRS and MACER provide similar improvement over COHEN, but QCRS incurs little computational overhead. Combining QCRS and MACER provides state-of-the-art certified radii.

Table 3: QCRS ACR results incorporating MACER. The models are trained using COHEN or MACER with (a)  $\sigma = .25$  and (b)  $\sigma = .50$ . The arrows indicate the comparison direction.

(a) $\sigma = 0.25$			
Test	Training		$\Rightarrow$ Improve
	COHEN	MACER	
Original	0.423	0.518	+22.5%
<b>QCRS</b>	0.512	0.715	+39.7%
$\downarrow$ Improve	+21%	+38%	<b>+69%</b>

(b) $\sigma = 0.50$			
Test	Training		$\Rightarrow$ Improve
	COHEN	MACER	
Original	0.534	0.669	+25.3%
<b>QCRS</b>	0.662	0.786	+18.7%
$\downarrow$ Improve	+24%	+17.5%	<b>+47.2%</b>

comparison. The last row and the last column show the relative improvement, as indicated by the annotated arrows. The bottom right value in the tables is the overall improvement. As Table 3 shows, for the model trained by  $\sigma = .25$ , COHEN achieves 0.423 ACR, and MACER enhances this ACR to 0.518, roughly 22.5%. Next, our proposed QCRS improves MACER ACR from 0.518 to 0.715, roughly 38%. Therefore, QCRS and MACER together can significantly boost the original Cohen’s RS roughly 69%. Similarly, for the model trained by  $\sigma = .50$ , QCRS and MACER enhance Cohen’s RS from 0.534 to 0.786, approximately +47.2%.

On the other hand, we can observe that the proposed method and MACER improves the original COHEN to 0.512 and 0.518, respectively. That is to say, the proposed method can enlarge the certified region to the extent that MACER does, but it does not need any training procedure. Note that nowadays dataset becomes larger and larger, re-training may be computationally prohibited. Thus, the proposed method benefits from its efficient workflow. It enlarges certified radius with negligible cost.

## 5.4 Computational Cost

We briefly analyze the computational cost compared to COHEN. The sigma searching region of Algorithm 1 is  $0.5 - 0.12 = 0.38$ . Because the convergence rate of Algorithm 1 is  $\frac{\sigma_{max} - \sigma_{min}}{2^t} \geq |\sigma_t - \sigma^*|$ , if  $t \geq 6$ , we can achieve 0.006-optimal, i.e.,  $|\sigma - \sigma^*| < 0.006$ . As for the gradient computation, it requires 1,000 forward propagations for each iteration. Thus, we roughly require additional 6,000 forward propagations for each data point to achieve the optimal sigma value. The standard RS needs 100,000 forward propagations, so the overhead of the proposed QCRS is approximately 6%. Empirically, we observe an approximately 7% overhead as Table 1 illustrates.

We also briefly analyze the computational cost of DDRS [Alfarra *et al.*, 2022], DSRS [Li *et al.*, 2022], and Insta-RS [Chen *et al.*, 2021]. DDRS uses the radius as their objective function and directly employ gradient descent to optimize the radius. It needs to take the gradient of the radius several times to update the sigma value, which requires multiple back propagations. In addition, before taking the gradient, DDRS needs to use MC sampling to compute the radius, which takes several forward propagations and is time-consuming. Furthermore, it maintains a memory bank, resulting in a high computational cost. Therefore, we can expect the time cost of DDRS to be significantly higher than that of the proposed QCRS. As for DSRS, the authors claim that the running time is roughly the same as Cohen’s method [Li *et al.*, 2022]. Thus, both DSRS and QCRS incur insignificant overhead, but QCRS compares favorably to DSRS in ACR, as Table 2 shows. Finally, Insta-RS employs multi-start gradient descent, so its computational cost is the highest among the methods considered in this paper.

## 6 Conclusion

In this work, we exploit and prove the quasiconcavity of the sigma-radius curve. The  $\sigma$ -SQC condition is general and easy to satisfy. Therefore, most data points (approximately 99%) conform to this condition. Based on the  $\sigma$ -SQC condition, we develop an efficient input-specific method called **QCRS** to efficiently find the optimal  $\sigma$  used for building the smoothed classifier, enhancing the traditional randomized smoothing significantly. Unlike former inference-time randomized smoothing methods that suffer from marginal improvement or high computational overhead, the proposed method enjoys better certification results and lower cost. We conducted extensive experiments on CIFAR-10 and ImageNet, and the results show that the proposed method significantly boosts the average certified radius with 7% overhead. Our method overcomes the trade-off in the RS inference phase between clean and robust accuracies on the radius-accuracy curve and eliminates the truncation effect. In addition, we combine the proposed QCRS with a training-based technique, and the results demonstrate the state-of-the-art average certified radii on CIFAR-10 and ImageNet. A direction for future work is to generalize the proposed method to  $\ell_p$  ball and different distributions. A better training approach for QCRS is also an interesting future research direction.

## References

- [Alfarra *et al.*, 2022] Motasem Alfarra, Adel Bibi, Philip HS Torr, and Bernard Ghanem. Data dependent randomized smoothing. In *Uncertainty in Artificial Intelligence (UAI)*, pages 64–74. PMLR, 2022.
- [Anderson and Sojoudi, 2022] Brendon G Anderson and Somayeh Sojoudi. Certified robustness via locally biased randomized smoothing. In *Learning for Dynamics and Control Conference*, pages 207–220. PMLR, 2022.
- [Boyd *et al.*, 2004] Stephen Boyd, Stephen P Boyd, and Lieven Vandenberghe. *Convex optimization*. Cambridge university press, 2004.
- [Carlini and Wagner, 2018] Nicholas Carlini and David Wagner. Audio adversarial examples: Targeted attacks on speech-to-text. In *2018 IEEE security and privacy workshops (SPW)*, pages 1–7. IEEE, 2018.
- [Chen *et al.*, 2021] Chen Chen, Kezhi Kong, Peihong Yu, Juan Luque, Tom Goldstein, and Furong Huang. Instars: Instance-wise randomized smoothing for improved robustness and accuracy. *arXiv preprint arXiv:2103.04436*, 2021.
- [Chen *et al.*, 2022] Ruoxin Chen, Jie Li, Junchi Yan, Ping Li, and Bin Sheng. Input-specific robustness certification for randomized smoothing. In *Proceedings of the AAAI Conference on Artificial Intelligence*, volume 36, pages 6295–6303, 2022.
- [Cohen *et al.*, 2019] Jeremy Cohen, Elan Rosenfeld, and Zico Kolter. Certified adversarial robustness via randomized smoothing. In *International Conference on Machine Learning (ICML)*, pages 1310–1320. PMLR, 2019.
- [Das *et al.*, 2018] Nilaksh Das, Madhuri Shanbhogue, Shang-Tse Chen, Fred Hohman, Siwei Li, Li Chen, Michael E Kounavis, and Duen Horng Chau. Shield: Fast, practical defense and vaccination for deep learning using jpeg compression. In *Proceedings of the 24th ACM SIGKDD International Conference on Knowledge Discovery & Data Mining*, pages 196–204, 2018.
- [Ehlers, 2017] Ruediger Ehlers. Formal verification of piecewise linear feed-forward neural networks. In *International Symposium on Automated Technology for Verification and Analysis*, pages 269–286. Springer, 2017.
- [Goodfellow *et al.*, 2014] Ian J Goodfellow, Jonathon Shlens, and Christian Szegedy. Explaining and harnessing adversarial examples. *arXiv preprint arXiv:1412.6572*, 2014.
- [Gowal *et al.*, 2018] Sven Gowal, Krishnamurthy Dvijotham, Robert Stanforth, Rudy Bunel, Chongli Qin, Jonathan Uesato, Relja Arandjelovic, Timothy Mann, and Pushmeet Kohli. On the effectiveness of interval bound propagation for training verifiably robust models. *arXiv preprint arXiv:1810.12715*, 2018.
- [Jeong *et al.*, 2021] Jongheon Jeong, Sejun Park, Minkyu Kim, Heung-Chang Lee, Doguk Kim, and Jinwoo Shin. Smoothmix: Training confidence-calibrated smoothed classifiers for certified adversarial robustness. In *ICML 2021 Workshop on Adversarial Machine Learning*, 2021.
- [Krizhevsky *et al.*, 2009] Alex Krizhevsky, Geoffrey Hinton, et al. Learning multiple layers of features from tiny images. *Citeseer*, 2009.
- [Kumar *et al.*, 2020a] Aounon Kumar, Alexander Levine, Soheil Feizi, and Tom Goldstein. Certifying confidence via randomized smoothing. *Advances in Neural Information Processing Systems (NeurIPS)*, 33:5165–5177, 2020.
- [Kumar *et al.*, 2020b] Aounon Kumar, Alexander Levine, Tom Goldstein, and Soheil Feizi. Curse of dimensionality on randomized smoothing for certifiable robustness. In *International Conference on Machine Learning (ICML)*, pages 5458–5467. PMLR, 2020.
- [Lecuyer *et al.*, 2019] Mathias Lecuyer, Vaggelis Atlidakis, Roxana Geambasu, Daniel Hsu, and Suman Jana. Certified robustness to adversarial examples with differential privacy. In *2019 IEEE Symposium on Security and Privacy (SP)*, pages 656–672. IEEE, 2019.
- [Levine and Feizi, 2021] Alexander J Levine and Soheil Feizi. Improved, deterministic smoothing for L1 certified robustness. In *International Conference on Machine Learning (ICML)*, pages 6254–6264. PMLR, 2021.
- [Levine *et al.*, 2020] Alexander Levine, Aounon Kumar, Thomas Goldstein, and Soheil Feizi. Tight second-order certificates for randomized smoothing. *arXiv preprint arXiv:2010.10549*, 2020.
- [Li *et al.*, 2022] Linyi Li, Jiawei Zhang, Tao Xie, and Bo Li. Double sampling randomized smoothing. In *International Conference on Machine Learning (ICML)*, pages 13163–13208. PMLR, 2022.
- [Madry *et al.*, 2017] Aleksander Madry, Aleksandar Makelev, Ludwig Schmidt, Dimitris Tsipras, and Adrian Vladu. Towards deep learning models resistant to adversarial attacks. *arXiv preprint arXiv:1706.06083*, 2017.
- [Mohapatra *et al.*, 2021] Jeet Mohapatra, Ching-Yun Ko, Lily Weng, Pin-Yu Chen, Sijia Liu, and Luca Daniel. Hidden cost of randomized smoothing. In *International Conference on Artificial Intelligence and Statistics*, pages 4033–4041. PMLR, 2021.
- [Nesterov, 2018] Yurii Nesterov. *Lectures on convex optimization*, volume 137. Springer, 2018.
- [Russakovsky *et al.*, 2015] Olga Russakovsky, Jia Deng, Hao Su, Jonathan Krause, Sanjeev Satheesh, Sean Ma, Zhiheng Huang, Andrej Karpathy, Aditya Khosla, Michael Bernstein, et al. Imagenet large scale visual recognition challenge. *International journal of computer vision (IJCV)*, 115(3):211–252, 2015.
- [Salman *et al.*, 2019] Hadi Salman, Jerry Li, Ilya Razenshteyn, Pengchuan Zhang, Huan Zhang, Sebastien Bubeck, and Greg Yang. Provably robust deep learning via adversarially trained smoothed classifiers. *Advances in Neural Information Processing Systems (NeurIPS)*, 32, 2019.



- [Samangouei *et al.*, 2018] Pouya Samangouei, Maya Kabkab, and Rama Chellappa. Defense-gan: Protecting classifiers against adversarial attacks using generative models. In *International Conference on Learning Representations (ICLR)*, 2018.
- [Shafahi *et al.*, 2019] Ali Shafahi, Mahyar Najibi, Mohammad Amin Ghiasi, Zheng Xu, John Dickerson, Christoph Studer, Larry S Davis, Gavin Taylor, and Tom Goldstein. Adversarial training for free! *Advances in Neural Information Processing Systems (NeurIPS)*, 32, 2019.
- [Súkeník *et al.*, 2021] Peter Súkeník, Aleksei Kuvshinov, and Stephan Günnemann. Intriguing properties of input-dependent randomized smoothing. *arXiv preprint arXiv:2110.05365*, 2021.
- [Szegedy *et al.*, 2013] Christian Szegedy, Wojciech Zaremba, Ilya Sutskever, Joan Bruna, Dumitru Erhan, Ian Goodfellow, and Rob Fergus. Intriguing properties of neural networks. In *International Conference on Learning Representations (ICLR)*, 2013.
- [Tjeng *et al.*, 2018] Vincent Tjeng, Kai Y Xiao, and Russ Tedrake. Evaluating robustness of neural networks with mixed integer programming. In *International Conference on Learning Representations (ICLR)*, 2018.
- [Wang *et al.*, 2022] Chien-Yao Wang, Alexey Bochkovskiy, and Hong-Yuan Mark Liao. Yolov7: Trainable bag-of-freebies sets new state-of-the-art for real-time object detectors. *arXiv preprint arXiv:2207.02696*, 2022.
- [Wong *et al.*, 2020] Eric Wong, Leslie Rice, and J Zico Kolter. Fast is better than free: Revisiting adversarial training. *arXiv preprint arXiv:2001.03994*, 2020.
- [Yang *et al.*, 2020] Greg Yang, Tony Duan, J Edward Hu, Hadi Salman, Ilya Razenshteyn, and Jerry Li. Randomized smoothing of all shapes and sizes. In *International Conference on Machine Learning (ICML)*, pages 10693–10705. PMLR, 2020.
- [Zhai *et al.*, 2019] Runtian Zhai, Chen Dan, Di He, Huan Zhang, Boqing Gong, Pradeep Ravikumar, Cho-Jui Hsieh, and Liwei Wang. Macer: Attack-free and scalable robust training via maximizing certified radius. In *International Conference on Learning Representations (ICLR)*, 2019.
- [Zhai *et al.*, 2022] Xiaohua Zhai, Alexander Kolesnikov, Neil Houlsby, and Lucas Beyer. Scaling vision transformers. In *Proceedings of the IEEE/CVF Conference on Computer Vision and Pattern Recognition (CVPR)*, pages 12104–12113, 2022.
- [Zhang *et al.*, 2020] Dinghui Zhang, Mao Ye, Chengyue Gong, Zhanxing Zhu, and Qiang Liu. Black-box certification with randomized smoothing: A functional optimization based framework. *Advances in Neural Information Processing Systems (NeurIPS)*, 33:2316–2326, 2020.

## Appendix

### A Comparison

The proposed QCRS method is novel in that it requires a much looser  $\sigma$ -SQC assumption and obtains the optimal sigma solution with a much faster convergence rate than prior work. We illustrate the detailed comparison to the gradient-based method. Table 4 compares QCRS to DDRS [Alfarra *et al.*, 2022], a gradient-based SOTA method for finding the optimal sigma.

	QCRS	DDRS
Assumption	$\sigma$ -SQC	concavity
Generality	high (99%)	low (7%)
Convergence	$\mathcal{O}((\frac{1}{2})^t)$	no
Back-propagation	no	yes
Time cost	low	high

Table 4: Detailed comparisons with DDRS.

For the generality of assumptions, almost all data points satisfy the  $\sigma$ -SQC condition, while only 7% of data points satisfy concavity. In addition, the proposed QCRS guarantees convergence, and the complexity is  $\log N$  to find the optimal solution on the  $N$ -grid. Furthermore, QCRS enjoys the advantages of computation. It does not employ back-propagation, making it computationally less expensive than DDRS.

### B Proof

In this section, we theoretically analyze the convergence of the proposed methods and provide proof. The convergence of the gradient-based method is also discussed.

Without loss of generality, we discuss convexity rather than concavity here. First, we prove Theorem 1 in the main paper as follows:

*Proof.* Let  $\sigma_t$  be the  $\sigma$  under  $t$  iterations. Suppose that  $R$  satisfies  $\sigma$ -SQC condition, and there exists a  $\sigma^* \in [\sigma_{min}, \sigma_{max}]$ . Then, for the first iteration  $\sigma_1 = \frac{\sigma_{max} + \sigma_{min}}{2}$ , we have

$$\frac{\sigma_{max} - \sigma_{min}}{2} \geq |\sigma_1 - \sigma^*|,$$

because  $\sigma_1$  is the midpoint of  $\sigma_{min}$  and  $\sigma_{max}$ . Without loss of generality, we assume  $\sigma_{min} \leq \sigma^* \leq \sigma_1$ . Thus, according to Algorithm 1,  $\sigma_2 = \frac{\sigma_{min} + \sigma_1}{2}$ , and

$$\frac{\sigma_{max} - \sigma_{min}}{2^2} \geq |\sigma_2 - \sigma^*|.$$

If we run  $t$  iteration, we can conclude that

$$\frac{\sigma_{max} - \sigma_{min}}{2^t} \geq |\sigma_t - \sigma^*|.$$

■

□

Therefore, to achieve  $\delta$ -optimal, the convergence rate of the proposed method is  $\mathcal{O}((\frac{1}{2})^t)$ .

Next, we further analyze the convergence of the gradient-based method.  $L$ -smoothness or  $\mu$ -strong convexity are necessary to guarantee convergence. We first show the convergence rate of  $L$ -smoothness:

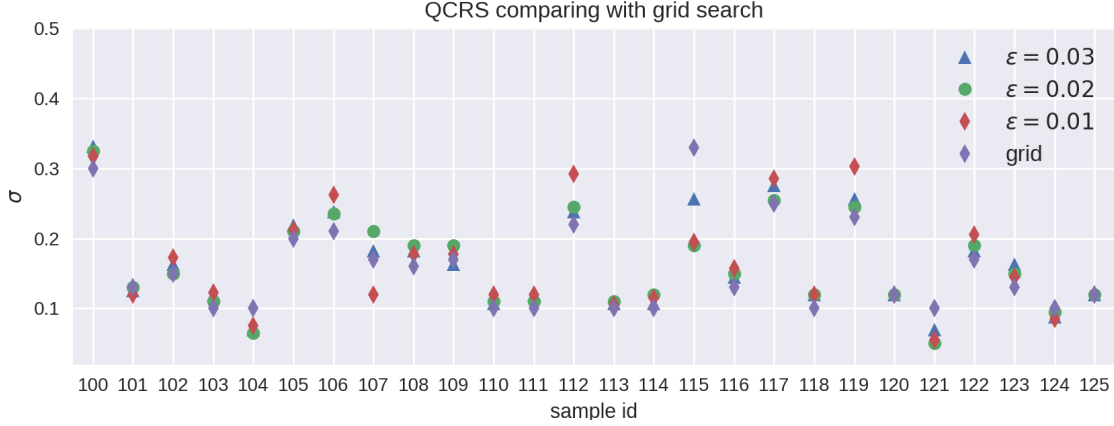


Figure 6: We demonstrate four sigma values found by different algorithms and parameters. The purple points represent sigma values found by grid search. The other points are sigma values found by the proposed QCRS. We tested different  $\varepsilon$  values, which indicate  $\varepsilon$ -optimal solutions. The  $\varepsilon$  values also serve as the terminal conditions of Algorithm 1.

**Theorem 2.** Suppose a function  $R(\sigma)$  is  $L$ -smooth for some  $L > 0$  with respect to  $\sigma$ . Then, if we run gradient descent for  $t$  iterations, it converges as follows [Nesterov, 2018]:

$$R(\sigma_t) - R(\sigma^*) \leq \frac{L|\sigma_1 - \sigma^*|^2}{2(t-1)}.$$

In addition, if both  $L$ -smoothness and  $\mu$ -strong convexity hold, the convergence rate is as follows:

**Theorem 3.** Suppose a function  $R(\sigma)$  is  $L$ -smooth and  $\mu$ -strongly convex for some  $L, \mu > 0$  with respect to  $\sigma$ , and  $\hat{\sigma}$  is the optimal sigma. Then, if we run gradient descent for  $t$  iterations, it converges as follows [Nesterov, 2018]:

$$|\sigma_t - \sigma^*|^2 \leq \left(\frac{L-\mu}{L+\mu}\right)^{(t-1)} |\sigma_1 - \sigma^*|^2.$$

Theorem 2 shows the convergence rate under the convex and  $L$ -smooth condition.  $R$  with  $L$ -smoothness can not guarantee  $\delta$ -optimal, i.e.,  $|\sigma^* - \sigma| \leq \delta$ . On the other hand, Theorem 3 shows the convergence rate under the  $L$ -smooth and  $\mu$ -convex condition, which is faster but stricter than Theorem 2. If we want to achieve  $\delta$ -optimal for  $\sigma$ , the convergence rate of  $\mathcal{O}\left(\left(\frac{L-\mu}{L+\mu}\right)^t\right)$ , where  $t$  is the number of iterations.

## C Error on sigma

We assume that the optimal sigma found by grid search is the true optimum. Therefore, we compare the optimal sigma found by QCRS with that found by grid search. We randomly selected some images and the results are shown in Fig. 6. The sigma found by QCRS is close to the sigma found by grid search.

## D Gradient Stability

The number of MC samples significantly affects the estimation of  $p_A(\sigma)$ . As shown in Fig. 7, if the sample number is 500, the possible interval is represented by the red region with a confidence level of  $1 - \alpha$ . The red region is very wide, causing uncertainty in the estimation of  $p_A(\sigma)$ , resulting in an

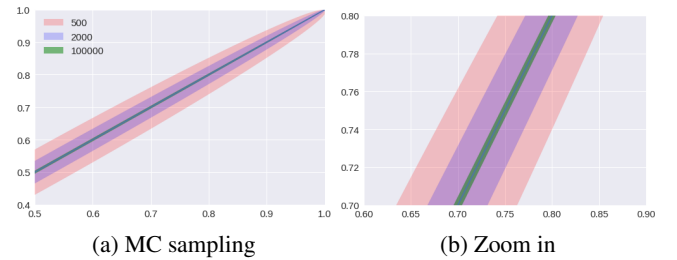


Figure 7: We plot the confidence interval of  $p_A(\sigma)$  with respect to  $p_A(\sigma)$ . The number of MC sampling significantly affects the confidence interval. Lower MC sample numbers result in wider confidence intervals. The red region in the figure represents the confidence interval of  $p_A(\sigma)$  with a  $1 - \alpha$  confidence level and 500 MC sampling number. It is wider than the one with 100,000 MC sampling number. This shows that the low MC sampling number makes the certified region uncertain. When estimating gradient values, if the value depends on MC sampling, the corresponding gradient will be unstable, making optimization difficult to converge. Prior work such as DDRS used a very low MC sampling number (as low as 8) when optimizing the sigma value, leading to unstable optimization.

unstable estimation. To minimize computational costs, previous work that relied on backpropagation often used low sample numbers, leading to an unstable computed gradient and potentially poor optimization of  $\sigma$ .